10.1109/ULTSYM.2015.0281

A Discrete Source Model for Simulating Bowl-Shaped Focused Ultrasound Transducers on Regular Grids: Design and Experimental Validation

Yan To Ling*†, Eleanor Martin*, and Bradley E. Treeby*‡
*Department of Medical Physics and Biomedical Engineering, University College London, London, UK
†Department of Electrical Engineering, The Chinese University of Hong Kong, Hong Kong, China
‡Email: b.treeby@ucl.ac.uk

***Abstract*—Accurately representing the behaviour of acoustic sources is an important part of ultrasound simulation. This is particularly challenging in ultrasound therapy where multi-element arrays are often used. Typically, sources are defined as a boundary condition over a 2D plane within the computational model. However, this approach is difficult to apply to arrays with multiple elements distributed over a non-planar surface. In this work, a grid-based discrete source model for single and multi-element bowl-shaped transducers is developed. The source model is defined as a symmetric, simply-connected surface with a single grid point thickness. Simulations using the source model with the open-source k-Wave toolbox are validated using the Rayleigh model and experimental measurements of a focused bowl transducer. The results show good agreement, even at very low grid resolutions. As the model only requires the geometry and drive signal, it allows modelling of multi-element transducers where measuring an input plane is not possible. This may be particularly useful for modelling hemispherical ultrasound arrays often used in transcranial applications.**

I. Introduction

Accurately representing source conditions is an important part of numerical simulation in ultrasound, particularly in high-intensity focused ultrasound (HIFU) and other ultrasound therapies where multi-element arrays are used [1, 2]. Typically, ultrasound sources are defined within computational models as boundary conditions defined over a 2D input plane [3]. These input planes are either measured experimentally [2, 4], or projected using analytical expressions [5]. However, for arrays with multiple elements distributed over a non-planar surface, there are two limitations with this approach. First, if the focal region is close to or within the bounding surface of the array (as is the case for hemispherical arrays used in transcranial applications [6]), it is difficult to define a single 2D plane over which the source can be measured and applied. Second, the input plane must be defined (i.e., measured or projected) for each set of drive conditions. This is a significant limitation when investigating the response of clinical HIFU systems, which may have hundreds or thousands of individual elements that are phased differently for each sonication [2]. One way in which these limitations can be overcome is to use an explicit source model. In this case, the response of the source is included within the model as the injection of mass or force at particular grid points with the computational mesh, rather than the imposition of a planar boundary condition. For finite difference and pseudospectral models, which are arguably the most commonly used numerical methods in ultrasound simulation [7], a regular Cartesian grid is generally used, and thus the source geometry must also conform to this mesh. In this work, a grid-based discrete source model for single and multi-element bowl-shaped transducers is developed, and validated against analytical models and experimental data.

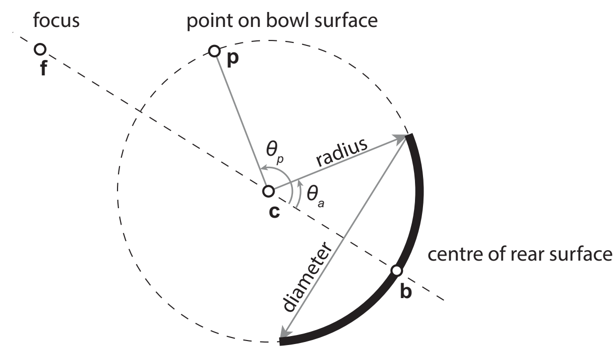

Fig. 1. Geometry of the discrete source model. Each bowl transducer is defined by the position of the rear surface $\mathbf{b}$, the radius of curvature, the diameter, and a point on the beam axis $\mathbf{f}$.

II. Discrete Source Model

A. Requirements

There are several requirements for the grid-based bowl-shaped source model. First, sources of the same radius of curvature and diameter facing the positive/negative x-direction, y-direction, or z-direction should be represented by the same shape and the same number of grid points. This means the sphere on which the bowl lies should have three axes of order-two rotational symmetry. Second, the source model should be singly connected (i.e., have only a single grid point thickness). This is to ensure that the acoustic field generated by the source is neither magnified or smoothed due to overlapping source points nor reduced due to discontinuities. The model is singly connected if for each grid point marked as part of the source, exactly 8 out of the 26 neighbouring points are also marked (with the exception of grid points along the outer rim of the source).

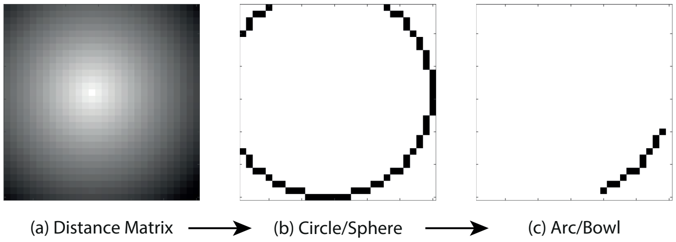

Fig. 2. Two-dimensional illustration of the steps used to create the discrete source model. First, a distance matrix is calculated containing the Euclidean distance from each point to the centre of the sphere on which the bowl lies (darker indicates larger distance). Next, the grid points where the distance is within 0.5 grid points of the radius of curvature are labelled. Finally, points that lie outside the arc angle of the bowl are removed.

B. Formulation

The geometry of the bowl-shaped source model is defined as shown in Fig. 1. Each transducer is defined by the position of the centre of the rear surface of the bowl $\mathbf{b}$ (analogous to the midpoint of an arc in 2D), the radius of curvature of the bowl, the diameter, any point on the beam axis $\mathbf{f}$ where $\mathbf{f} \neq \mathbf{b}$ (this defines the orientation of the source), and the overall size of the Cartesian grid in which the source is defined. Using these parameters, the position $\mathbf{c}$ of the centre of the sphere on which the bowl lies is calculated using

$$\mathbf{c} = \frac{\text{radius}}{\|\mathbf{f}-\mathbf{b}\|}\left(\mathbf{f}-\mathbf{b}\right)+\mathbf{b} \ . \tag{1}$$

A distance matrix is then created which contains the Euclidean distance from each point in the Cartesian grid to $\mathbf{c}$. An example in 2D is given in Fig. 2(a). A series of bi-directional line searches along each dimension of the distance matrix are then conducted (i.e., first along all the rows in each direction, then along the columns, etc). The grid points with Euclidean distance to the sphere centre within 0.5 grid points of the radius of curvature are then labelled. This results in a singly connected sphere (or circle in 2D) with the correct radius centred at $\mathbf{c}$. An example is shown in Fig. 2(b).

Next, the grid points within the sphere that do not form part of the bowl are removed. This is performed by calculating the angle θ_p between the vector from each grid point $\mathbf{p}$ on the sphere surface to the sphere centre $\mathbf{c}$, and the vector from the rear surface of the bowl $\mathbf{b}$ to the sphere centre using the geometric definition of the dot product

$$\theta_p = \cos^{-1}\left(\frac{(\mathbf{p}-\mathbf{c})\bullet(\mathbf{b}-\mathbf{c})}{\|\mathbf{p}-\mathbf{c}\|\,\|\mathbf{b}-\mathbf{c}\|}\right) \ . \tag{2}$$

The grid points for which θ_p is greater than the half arc angle θ_a, where

$$\theta_a = \sin^{-1}\left(\text{diameter}/\left(2\times\text{radius}\right)\right) \ , \tag{3}$$

are then removed. This leaves a symmetric and simply-connected bowl-shaped surface with a single grid point thickness. Functions to generate single and multiple bowls (in 3D) and single and multiple arcs (in 2D) using this approach were written in MATLAB. An example of a low resolution bowl and a multi-element hemispherical array containing 64 individual bowls (based on [6]) are shown in Fig. 3.

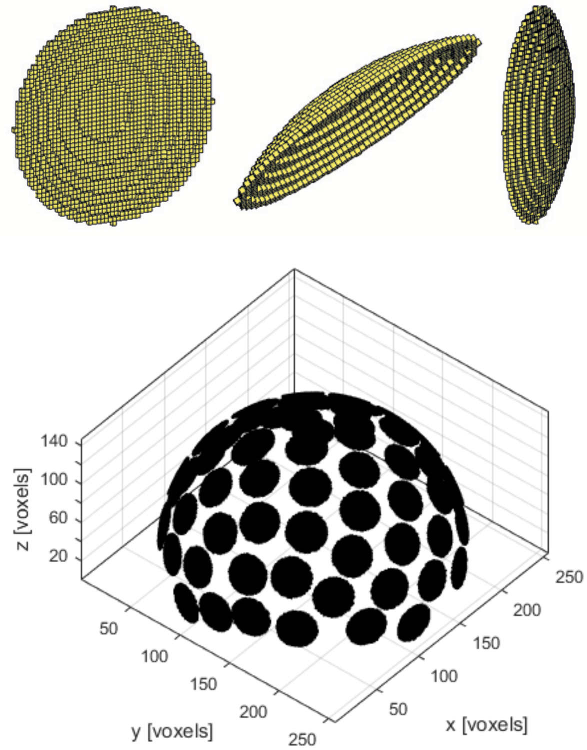

Fig. 3. (Top) Three views of a low resolution grid-based bowl transducer generated as described in Sec. II.B. The radius of curvature of the bowl is 100 grid points, and the diameter is 45 grid points. (Bottom) Example of a multi-element hemispherical transducer array containing 64 individual bowls.

III. Validation

A. Numerical Testing

To test the grid-based discrete bowl model, a series of simulations were performed using the open source k-Wave MATLAB toolbox [8]. This solves the acoustic equations on a regular Cartesian grid using a k-space pseudospectral scheme. The source geometry was based on the H-101 single element HIFU transducer (Sonic Concepts, WA, USA). This has a diameter of 64 mm, and a radius of curvature of 63.2 mm. The discrete bowl surface was calculated as described in Sec. II.B, and used to define the pressure source mask (`source.p_mask`) within k-Wave. The beam axis was aligned with the Cartesian grid, and the source was driven by a continuous wave sinusoid at 1.1 MHz assuming linear and lossless propagation. Simulations were repeated using grid discretisations from 2.2 points per wavelength (PPW) up to 10.8 PPW. This corresponds to grid sizes of $256 \times 128 \times 128$ up to $1280 \times 640 \times 640$ grid points. (While the numerical model can theoretically propagate waves up to the Nyquist limit of 2 PPW, in practice, a slightly higher PPW is needed for the perfectly matched layer to work correctly [9].)

The numerical model used in k-Wave is exact in the limit of wave propagation in a homogeneous and lossless medium [8]. This means changing the number of PPW only changes the discretisation of the source geometry, and not the accuracy of the numerical model. The representation of the bowl surface

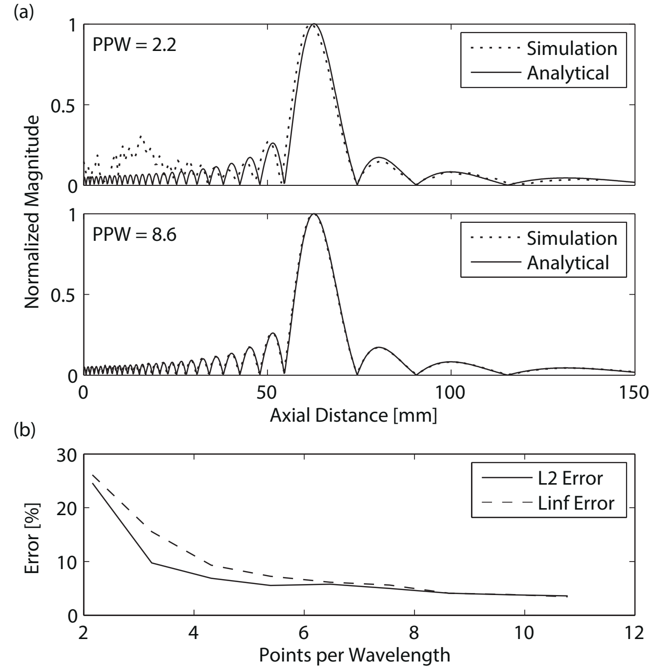

Fig. 4. (a) Axial pressure from a focused bowl transducer calculated using the discrete source model (dotted lines) and the Rayleigh model for two different points per wavelength (PPW). Even at very coarse grid resolutions close to the Nyquist limit, the main features of the pressure field are captured. (b) Convergence of the l_2 and l_∞ relative error norms with PPW.

as a series of discrete grid points on the Cartesian grid gives rise to staircasing errors [10, 11]. In particular, for low grid resolutions, the discrete source points are further away from the ideal bowl, which can affect the structure of the generated acoustic waves, particularly in the near-field.

The simulations were run using the parallelised C++ version of k-Wave [12]. For each simulation, the steady state pressure amplitude was recorded and compared with the pressure predicted by the Rayleigh model [13]. Results for the on-axis pressure for 2.2 and 8.6 PPW are shown in Fig. 4(a). The convergence of the relative l_2 and l_∞ error norms with the number of PPW is shown in Fig. 4(b). The errors converge very rapidly, and by 5 PPW, both error norms are below 10% (this level of uncertainty is typical of hydrophone calibrations). Even at very low PPW close to the Nyquist limit, the main features of the beam are still captured by the model. As expected, the biggest discrepancies are in the near-field region close to the source.

B. Experimental Testing

In addition to numerical testing, simulations using the source model were compared with experimental measurements made using a bowl-shaped HIFU transducer. The acoustic pressure field generated by a H-101 transducer was measured in a tank of deionized water (at 23.8 $\pm$ 0.1 °C) with a 0.2 mm needle hydrophone (Precision Acoustics, Dorchester, UK) as shown in Fig. 5. The transducer was driven by a signal generator (33522A, Agilent Technologies, Santa Clara, CA, USA) connected via a 75 W power amplifier (A075, E&I, Rochester, NY, USA) and impedance matching network. The drive signal was a 1.1 MHz sinusoidal burst containing 35-cycles at a pulse repetition frequency of 100 Hz, and an RMS voltage of 8.25 V. The hydrophone was positioned using a scanning tank (Precision Acoustics, Dorchester, UK) with two computer controlled translation stages [14]. This was used to acquire a 36 $\times$ 36 mm planar field scan perpendicular to the beam axis at a distance of 42.5 mm from the rear surface of the transducer bowl. Signals were digitised with a spatial step size of 300 μm via an oscilloscope (DSO-X 3024A, Agilent Technologies, Santa Clara, CA, USA) using a sampling frequency of 800 MHz and 32 averages.

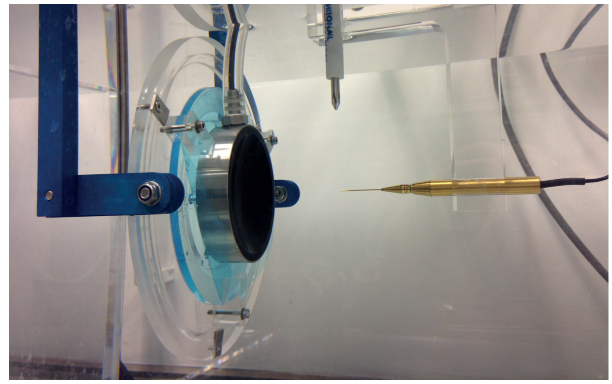

Fig. 5. Photograph of the experimental setup showing the bowl-shaped H-101 transducer and the 0.2 mm needle hydrophone within the scanning tank.

The experimental data was projected to other positions in the field via linear acoustic holography. Simulations based on the discrete bowl model were also performed with the nominal bowl dimensions and drive conditions matching the experimental setup. Axial and lateral beam plots centred on the transducer focus are shown in Fig. 6(a). Corresponding axial and lateral profiles are shown in Fig. 6(b). There is generally good agreement between the experimental and simulation results, particularly in the lateral profile, and the shape and position of the main beam. There are some discrepancies between the two fields in the pre and post focal regions of the axial profile. Given the excellent agreement shown in Fig. 4, this is most likely due to the diameter and curvature of the physical transducer not matching the values used in the simulation, or a slight misalignment in the experimental measurement.

C. Source Scaling

In both the numerical and experimental comparisons, the axial pressures are normalised to the peak values. This avoids any issues with scaling the numerical drive signal to achieve the correct surface and focal pressures. However, the staircased representation of the source geometry also introduces a scaling issue due to the different density of grid points in grid and diagonal directions. For example, a horizontal line tilted at 45° to the grid axis will contain a factor of $\sqrt{2}$ fewer grid points per unit length than a horizontal line aligned with grid axis. This disparity results in the generated acoustic pressure being a factor of $\sqrt{2}$ smaller. This can be approximately corrected

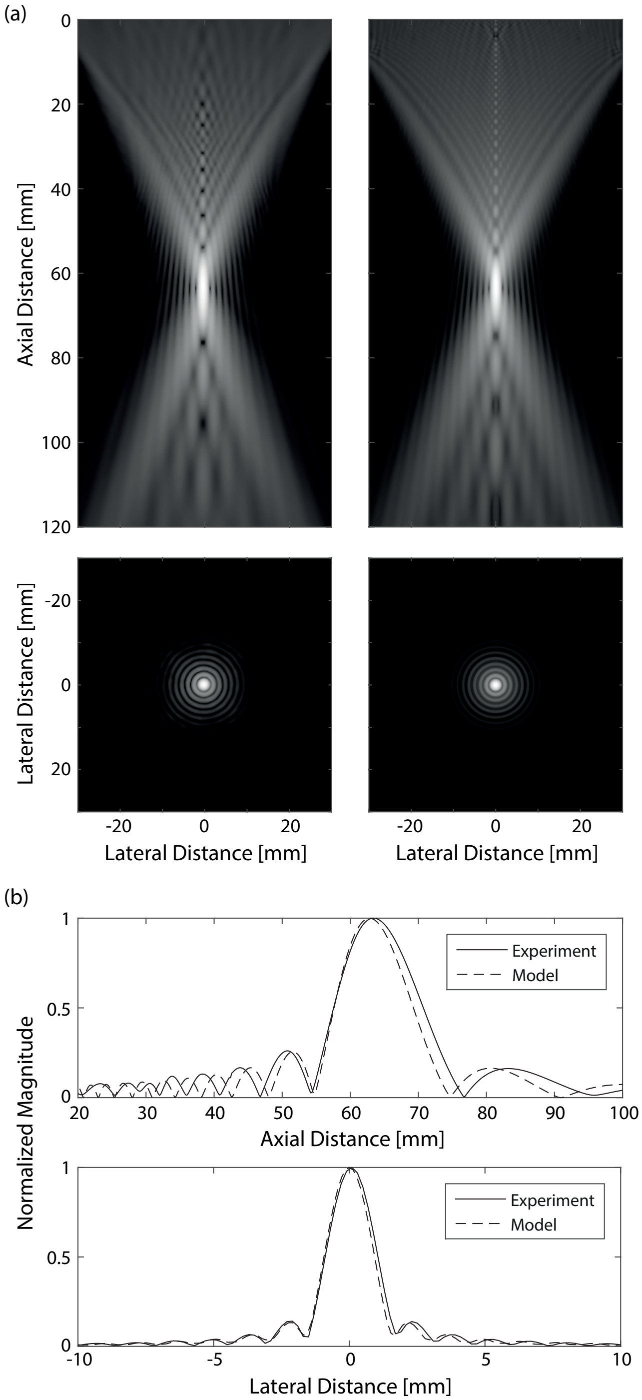

Fig. 6. Comparison between experimental measurements and simulations of a H-101 focused bowl transducer in water. (a) Axial and lateral beam patterns centred on the transducer focus, and (b) corresponding axial and lateral profiles.

for by scaling the individual drive signals for each grid point by the average distance to the neighbouring grid points that also form part of the transducer surface.

IV. Summary

A method for generating a discrete bowl shape on a regular Cartesian grid is presented. This can be used to directly model bowl shaped transducers in ultrasound simulations based on a Cartesian grid in place of planar boundary conditions. The acoustic fields generated using these geometries agree well with the fields predicted by the Rayleigh model and experimentally measured from bowl-shaped transducers. The functions (called `makeBowl`, `makeMultiBowl`, `makeArc` and `makeMultiArc`) will be made available with the next release of the k-Wave toolbox [8].

Acknowledgment

This work was supported in part by the Engineering and Physical Sciences Research Council (EPSRC), UK.

References

[1] P. Gélat, G. ter Haar, and N. Saffari. Modelling of the acoustic field of a multi-element HIFU array scattered by human ribs. *Physics in Medicine and Biology*, 56(17):5553–5581, 2011.

[2] W. Kreider, P. Yuldashev, O. A. Sapozhnikov, N. Farr, A. Partanen, M. R. Bailey, and V. A. Khokhlova. Characterization of a multi-element clinical HIFU system using acoustic holography and nonlinear modeling. *IEEE Trans. Ultrason. Ferroelectr. Freq. Control*, 60(8):1683–1698, 2013.

[3] O. A. Sapozhnikov, S. A. Tsysar, V. A. Khokhlova, and W. Kreider. Acoustic holography as a metrological tool for characterizing medical ultrasound sources and fields. *J. Acoust. Soc. Am.*, 138(3):1515–1532, 2015.

[4] M. S. Canney, M. R. Bailey, L. A. Crum, V. A. Khokhlova, and O. A. Sapozhnikov. Acoustic characterization of high intensity focused ultrasound fields: A combined measurement and modeling approach. *J. Acoust. Soc. Am.*, 124(4):2406, 2008.

[5] X. Zeng and R. J. McGough. Optimal simulations of ultrasonic fields produced by large thermal therapy arrays using the angular spectrum approach. *J. Acoust. Soc. Am.*, 125(5):2967–2977, 2009.

[6] G. T. Clement, J. Sun, T. Giesecke, and K. Hynynen. A hemisphere array for non-invasive ultrasound brain therapy and surgery. *Phys. Med. Biol.*, 45(12):3707–19, 2000.

[7] M. D. Verweij, B. E. Treeby, K. W. A. van Dongen, and L. Demi. Simulation of Ultrasound Fields. In A. Brahme, editor, *Comprehensive Biomadical Physics*, volume 2, chapter 2.19, pages 465–500. Elsevier, Amsterdam, 2014.

[8] B. E. Treeby and B. T. Cox. k-Wave: MATLAB toolbox for the simulation and reconstruction of photoacoustic wave fields. *J. Biomed. Opt.*, 15(2):021314, 2010.

[9] J. L. Robertson, B. T. Cox, and B. E. Treeby. Quantifying numerical errors in the simulation of transcranial ultrasound using pseudospectral methods. In *IEEE International Ultrasonics Symposium*, pages 2000–2003, 2014.

[10] J. Van Aken and M. Novak. Curve-drawing algorithms for raster displays. *ACM Transactions on Graphics*, 4(2):147–169, 1985.

[11] E. Andres. Discrete circles, rings and spheres. *Computers & Graphics*, 18(5):695–706, 1994.

[12] J. Jaros, A. P. Rendell, and B. E. Treeby. Full-wave nonlinear ultrasound simulation on distributed clusters with applications in high-intensity focused ultrasound. *Int. J. High Perf. Comput. Appl.*, 2015.

[13] R. S. C. Cobbold. *Foundations of Biomedical Ultrasound*. Oxford University Press, New York, 2007.

[14] K. Wang, E. Teoh, J. Jaros, and B. E. Treeby. Modelling nonlinear ultrasound propagation in absorbing media using the k-Wave Toolbox: Experimental Validation. In *IEEE International Ultrasonics Symposium*, pages 523–526, 2012.